Performance Limits With Preview Information and Actuator Rate Constraints

Peter Seiler, Ahmet Arda Ozdemir, and Gary J. Balas

***Abstract*— This paper considers the limits of disturbance rejection performance with preview information subject to actuator rate constraints. A one-state, continuous-time optimal control problem is formulated to investigate these limits. The optimal control action which minimizes the peak tracking error is explicitly characterized using Lagrange duality theory. In addition, the optimal tracking performance as a function of preview time is provided. There is a fundamental preview time beyond which no performance improvements are obtained.**

I. Introduction

Actuator rate constraints place limits on the speed of response and performance of a feedback system. In particular, the rate constraints prevent the system from rejecting rapidly changing disturbances. In some cases, a preview measurement of the disturbance is available and can be used to partially overcome the actuator rate constraints. For example, LIDAR measurements of the incoming wind field have been investigated for wind turbine pitch control [6], [7], [5], [2], [3], [10]. As another example, the road profile can be measured with a forward-mounted radar on an off-road vehicle. This preview information can be incorporated into an active suspension controller [1].

This paper considers the limits of disturbance rejection performance with preview information subject to actuator rate constraints. An optimal, disturbance rejection problem is formulated in Section III. The formulation is in continuous-time and assumes first order plant dynamics. The disturbance rejection performance depends on the amount of preview time. Next, Section IV summarizes the optimal input and state response for the case where the system is marginally stable. This special case yields simple formulas that provide rough guidelines for how the optimal performance varies as a function of preview time. In addition, this special case provides the basic intuition for the following result: there exists a preview time beyond which no performance improvement is obtained. This result is proved in Section V using the Lagrange duality theory for vector space optimization [8].

There is a large body of literature on preview control. A brief, by no means complete, list of work includes feedback control design based on linear quadratic [12], H_∞ [4], and H_2 [9] costs. This paper uses the peak L_∞ norm to measure tracking errors and derives explicit formulas for the optimal open-loop control actions. In addition, the derivation in this paper considers the effect of actuator rate limits.

Aerospace and Engineering Mechanics Department, University of Minnesota, seiler@aem.umn.edu, arda@aem.umn.edu and balas@umn.edu.

II. Notation

The notation aligns with that used in [8]. $C^n[a,b]$ is the normed linear space of vector-valued, continuous functions $f:[a,b]\to\mathbb{R}^n$. The norm on $C^n[a,b]$ is given by $\|f\|_\infty := \max_{a\le t\le b}\max_{1\le i\le n}|f_i(t)|$. The superscript n is dropped for scalar functions, i.e. $C[a,b]$ denotes scalar continuous functions. Similarly, $C^n[a,\infty)$ is the space of vector-valued, uniformly-bounded, continuous functions $f:[a,\infty)\to\mathbb{R}^n$ with the norm $\|f\|_\infty := \sup_{t\ge a}\max_{1\le i\le n}|f_i(t)|$.

The total variation of a function $f:[a,b]\to\mathbb{R}$ is defined as $TV(f) := \sup\sum_{i=1}^n |f(t_i)-f(t_{i-1})|$ where the sup is over all finite partitions $a=t_0<t_1<\cdots<t_n=b$ of the interval $[a,b]$. $NBV[a,b]$ is the normalized space of functions with bounded total variation on $[a,b]$. The functions $f\in NBV[a,b]$ are normalized such that f is right continuous and $f(a)=0$. $NBV^n[a,b]$ denotes the space of functions $f:[a,b]\to\mathbb{R}^n$ such that each $f_i\in NBV[a,b]$.

Define the positive cone $P\subset C^n[a,b]$ by $P := \{f\in C^n[a,b] \ : \ f_i(t)\ge 0 \ \forall t\in[a,b]\}$. Denote $f\ge 0$ if $f\in P$ and $f\le 0$ if $-f\in P$. Moreover, denote $f>0$ if f is an interior point of P, i.e. $f_i(t)>0 \ \forall t\in[a,b]$. Finally, define the positive cone $P^*\subset NBV^n[a,b]$ as the subset of functions f such that f_i is a non-decreasing on $[a,b]$. Again, denote $f\ge 0$ if $f\in P^*$ and $f\le 0$ if $-f\in P^*$.

III. Problem Formulation

Consider the first-order system:

$$\dot{x}(t) = -ax(t) + bu(t) + d(t) \tag{1}$$

where $x\in\mathbb{R}$ is the state, $u\in\mathbb{R}$ is the control input, and $d\in\mathbb{R}$ is the disturbance. Assume the system is marginally or strictly stable ($a\ge 0$). In addition, assume without loss of generality that $b>0$. The control objective is to regulate $x(t)$ to zero. The disturbance is "matched" in Equation 1 and hence it can be perfectly canceled by setting $u(t) = -\frac{d(t)}{b}$. However, perfect cancellation is not possible if the actuator is subject to rate constraints and the disturbance is rapidly changing. In some cases preview information of the disturbance is available for the controller. In other words, the controller at time t may have access to a measurement or estimate of $d(\tau)$ for $\tau>t$. Intuitively, preview information can be used to partially overcome the disturbance rejection limitations imposed by actuator rate constraints.

The following optimal control problem is used to study the disturbance rejection performance as a function of the

preview time and the actuator rate constraint.

$$p(T) := \inf_{\dot{u}\in C[0,\infty)} \|x\|_\infty \quad (2)$$
$$\text{subject to:}$$
$$\dot{x}(t) = -ax(t) + bu(t) + d_T(t)$$
$$x(0) = 0,\ u(0) = 0,\ |\dot{u}(t)| \le r$$
$$d_T(t) := \begin{cases} 0 & \text{if } t < T \\ \bar{d} & \text{if } t \ge T \end{cases}$$

In words, the system is initialized at the equilibrium $x(0) = 0$ and is disturbed by a step of magnitude $\bar{d}$ at time T. For concreteness, assume $\bar{d} > 0$. The objective is to design the optimal input that minimizes the peak deviation in x. u is rate constrained and hence the disturbance cannot be perfectly canceled. However, the formulation allows u to anticipate the disturbance, i.e. u can begin moving at $t = 0$ to cancel the step disturbance at $t = T$. This models a situation in which the controller has a measurement of the disturbance with T seconds of preview. $p(T)$ denotes the optimal performance as a function of the preview time T. The tracking performance p is a monotonic function of the preview time: $T' \ge T \Rightarrow p(T') \le p(T)$. This follows because any feasible solution for preview time T can be time-shifted to construct a feasible solution for $T' \ge T$ that achieves the same cost.

A concrete example for this problem formulation is rotor speed control for a wind turbine. At high (Region 3) wind speeds, the tower/blade structural loads are controlled by pitching the blades in response to wind gusts. The blade pitch actuators have restrictive rate limits due to the large blade inertia. As a result, it is not possible to respond to fast changing wind gusts. The use of preview information, e.g. LIDAR measurements of the incoming wind field, has been investigated to improve the load attenuation [6], [7], [5], [2], [3], [10]. For a wind turbine, Equation 1 represents the dominant rotor dynamics linearized about an operating wind speed. In this case, $x(t)$ denotes the rotor speed (rad/sec), $u(t)$ denotes the collective blade pitch angle (deg), and $d(t)$ denotes the wind speed deviation (m/sec). The optimal control problem in Equation 2 aims to minimize the peak variations in rotor speed due to a step wind gust. This one-state, optimal control formulation is too simplified to make a detailed assessment of the load reduction performance. In particular, the dynamics neglect the tower and blade bending modes. In addition, the step wind gust disturbance is only a rough approximation of the effects of the wind field. Nevertheless, rotor speed variations are well correlated with the various structural loads. Eliminating sharp peaks in rotor speed typically leads to reduced blade, tower and gearbox loads. Thus the simple rotor speed problem in Equation 2 can be used to understand the basic performance trends.

IV. Optimal Response For $a = 0$

This section describes the optimal response as a function of preview time T for the special case $a = 0$. This case provides the basic intuition for the main result derived for $a > 0$. In addition, these results yield simple formulas that provide guidelines for systems with small damping ($a \approx 0$). Due to space restrictions, proofs of optimality are not given. However, they can be derived using Lagrange duality theory similar to the approach taken in the next section.

A. No Preview: $T = 0$

If there is no preview ($T = 0$) then the optimal response is to ramp the control input at its maximum rate $\dot{u} = -r$ until u cancels the disturbance. It takes $T^* := \frac{\bar{d}}{rb}$ seconds to ramp the input u from 0 to $-\frac{\bar{d}}{b}$. Define the input:

$$u_0(t) = \begin{cases} -rt & \text{if } t < T^* \\ -\frac{\bar{d}}{b} & \text{if } t \ge T^* \end{cases} \quad (3)$$

Integration of the system dynamics (Equation 1) with $a = 0$ yields the trajectory:

$$x_0(t) = \begin{cases} \bar{d}t - \frac{brt^2}{2} & \text{if } t < T^* \\ \frac{\bar{d}^2}{2rb} & \text{if } t \ge T^* \end{cases} \quad (4)$$

Thus the minimal cost for the optimal control problem (Equation 2) with no preview is given by $p(0) = \frac{\bar{d}^2}{2rb}$. One technical issue is that the optimal control problem is formulated with $\dot{u} \in C[0,\infty)$. This formulation is required to apply the Lagrange duality theory in the next section. The u_0 in Equation 3 has $\dot{u}_0$ change discontinuously from $-r$ to 0 at $t = T^*$. Thus $\dot{u}_0 \notin C[0,\infty)$ for this input. However, there are continuous functions $\dot{u}$ that yield an input arbitrarily close to u_0 and a cost arbitrarily close to $p(0)$.[1]

B. Small Preview: $T \le \left(\sqrt{2} - 1\right) T^*$

For "small" preview times, the optimal input is still given by $u_0(t)$ in Equation 3. Specifically, $u_0(t)$ is optimal for preview times that satisfy $T \le \left(\sqrt{2} - 1\right) T^*$. Figure 1 shows the state responses with the optimal input $u_0(t)$ for three different "small" preview times. The responses are generated for the specific data $b = 1$, $r = 16$, and $\bar{d} = 16$. The solid line in Figure 1 is the response $x_0(t)$ for no preview (Equation 4). For this data, $T^* = 1$ sec and the minimal cost with no preview is $p(0) = 8$. The dashed and dash-dotted lines are the optimal responses for $T = 0.2$ and $T = 0.4$. The vertical dotted lines at $t = 0.2$ and $t = 0.4$ denote the time of the step disturbance for these two responses. The last vertical dotted line is at $T^* = 1$. All three trajectories achieve their peak magnitude at $t = T^*$ and have $\dot{x}(t) = 0$ for $t \ge T^*$.

For $T = 0.2$, the state trajectory is $-\frac{brt^2}{2}$ prior to the onset of the step disturbance. At $t = 0.2$, the state trajectory reverses direction due to the step disturbance and eventually reaches a steady state at $x(T^*) = 4.8$. The preview has two benefits. First, the control input is able to partially overcome the rate limit by ramping toward $-\frac{\bar{d}}{b}$ before the step disturbance occurs. Second, the initial negative motion of the state leaves the system in a better position to absorb the disturbance. In particular, the large positive peak at $x(T^*)$ is reduced because disturbance must first overcome the negative

[1] Inputs with discontinuous $\dot{u}$ will be used in the remainder of the paper with the same understanding. That is, a continuous $\dot{u}$ can be constructed to achieve a cost arbitrarily close to that achieved by the discontinuous $\dot{u}$.

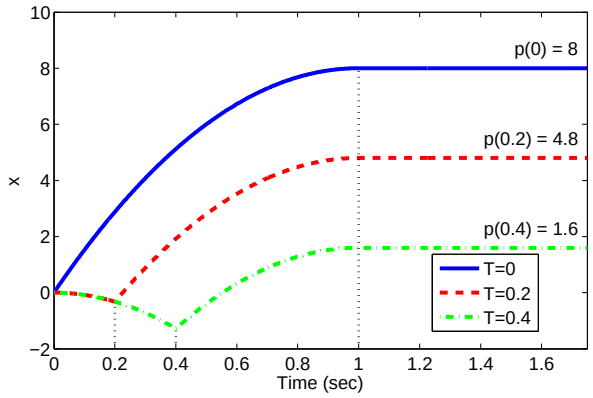

Fig. 1. Time responses of $x(t)$ for "small" preview times

value of $x(T)$ at the time of the step disturbance. As a result the optimal cost is reduced from $p(0) = 8$ to $p(0.2) = 4.8$.

The response for $T = 0.4$ shows a similar trend with the cost further reduced to $p(0.4) = 1.6$. Note that, for $T = 0.4$, the negative motion of the state trajectory prior to the disturbance reaches $x(T) = -1.28$. This is almost the same magnitude as $x(T^*) = 1.6$. As the preview time is further increased, the state at the time of the step disturbance, $x(T)$, continues to become more negative (larger in magnitude). In addition, $x(T^*)$ continues to decrease in magnitude. This trend continues until T becomes large enough that $|x(T)| = |x(T^*)|$. This happens precisely when $T = (\sqrt{2}-1)T^*$. For $T > (\sqrt{2}-1)T^*$, u_0 is no longer optimal because the negative peak at $x(T)$ dominates the cost.

C. Moderate Preview: $\left(\sqrt{2}-1\right)T^* < T \leq T^*$

For "moderate" preview times $(\sqrt{2}-1)T^* < T \leq T^*$, the optimal input is of the form:

$$u_T(t) = \begin{cases} +rt & \text{if } t < t_1 \\ -r(t-2t_1) & \text{if } t_1 \leq t < 2t_1 + T^* \\ -\frac{\bar{d}}{b} & \text{if } t \geq 2t_1 + T^* \end{cases} \quad (5)$$

where $t_1 := \frac{T^2+2TT^*-T^{*2}}{4(T+T^*)}$. The subscript in u_T denotes that the optimal input depends on T through the parameter t_1. For $t \leq t_1$ the optimal input u_T ramps at maximum rate in the wrong direction, i.e. away from the value $-\frac{\bar{d}}{b}$ required to cancel the disturbance. Then it ramps at maximum rate in the other direction until it reaches $-\frac{\bar{d}}{b}$. As noted above, the optimal cost for preview time $T = (\sqrt{2}-1)T^*$ becomes constrained by the negative peak at $x(T)$. The magnitude of $x(T)$ is reduced by ramping initially in the wrong direction.

Figure 2 shows the state response and optimal input $u_T(t)$ for three different "moderate" preview times. The solid, dashed, and dash-dotted lines are the responses for $T = 0.6$, 0.8, and 1.0. The responses are again generated for the specific data $b = 1$, $r = 16$, and $\bar{d} = 16$. The vertical dotted lines denote specific times related to the trajectory for $T = 1.0$ and will be discussed further below. All three trajectories have $\dot{x}(t) = 0$ for $t \geq 2t_1 + T^*$. For each preview time the state trajectory $x(t)$ achieves the peak magnitude $p(T)$ at both $t = T$ and $t = 2t_1 + T^*$. In other words, the value of t_1 is chosen to balance both the negative peak at $x(T)$ and the positive peak at $x(2t_1 + T^*)$.

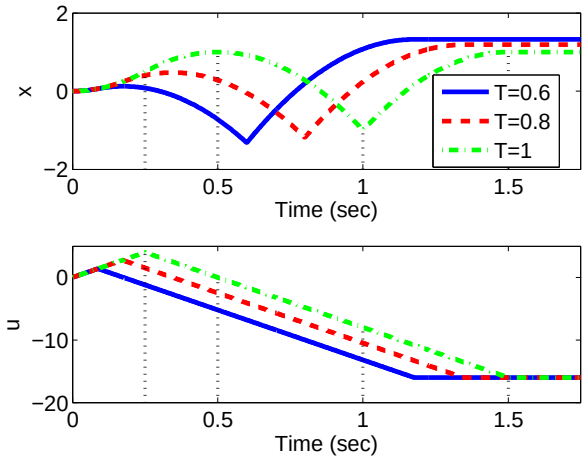

Fig. 2. Time responses of $x(t)$ and $u(t)$ for "moderate" preview times

For each trajectory the optimal control u_T is positive for $t < 2t_1$. This causes $x(t)$ to initially move in the positive direction and achieve a local maximum at $x(2t_1)$. As the preview time T increases, $x(2t_1)$ becomes more positive while the magnitudes of $x(T)$ and $x(2t_1 + T^*)$ are both reduced. When $T = T^*$ the first positive peak at $t = 2t_1$ satisfies $|x(2t_1)| = |x(T)| = |x(2t_1 + T^*)|$. For $T > T^*$, the input u_T in Equation 5 is no longer optimal because the magnitude of $x(2t_1)$ dominates the cost. For the given data, $T^* = 1.0$ and hence the dash-dotted curve in Figure 2 represents the optimal response for the limiting case of "moderate" preview ($T = T^*$). The four vertical dotted lines in each subplot are drawn at the times t_1, $2t_1$, T, and $2t_1+T^*$ for this response. The optimal input u shown in the bottom subplot changes from $\dot{u} = +r$ to $\dot{u} = -r$ at t_1. The top subplot shows that the optimal $x(t)$ for $T = 1.0$ achieves its maximum magnitude at times $2t_1$, T, and $2t_1 + T^*$.

D. Long Preview: $T > T^*$

For $T > T^*$ one might suspect that $p(T)$ can be further reduced by pre-pending the control action $u_{T^*}(t)$ with an initial negative ramp. This might simultaneously reduce the magnitudes of $x(2t_1)$, $x(T)$, and $x(2t_1+T^*)$ which constrain the performance for $T = T^*$. In actuality, no further improvement can be obtained for $T > T^*$, i.e. $p(T) = p(T^*)$ for $T \geq T^*$. The optimal input for $T > T^*$ is not unique but one choice is given by:

$$u_T(t) = \begin{cases} 0 & \text{if } t < T - T^* \\ u_{T^*}\left(t - (T - T^*)\right) & \text{if } t \geq T - T^* \end{cases} \quad (6)$$

where u_{T^*} is the optimal input given by Equation 5 for $T = T^*$. This choice wastes the first $T - T^*$ seconds of preview by leaving the input at zero and then executes the control action u_{T^*} once T^* seconds of preview remains. It can be shown that the minimal cost is $p(T) = \frac{\bar{d}^2}{16rb}$ for $T \geq T^*$.

E. Summary

The solution to the optimal control problem (Equation 2) for $a = 0$ is summarized in Table I. Figure 3 shows the optimal cost versus preview time. In this figure the preview time on the horizontal axis has been normalized by T^* and the cost on the vertical axis has been normalized by $p(0)$. $T^* = \frac{\bar{d}}{rb}$ is a fundamental preview time beyond which no additional performance improvements are obtained. In addition, $p(0) = \frac{\bar{d}^2}{2rb}$ and $p(T^*) = \frac{\bar{d}^2}{16rb}$. Thus, preview information can, at best, reduce the peak tracking error by a factor of eight compared to the performance with no preview. Finally, the use of preview has the largest impact for $T \leq (\sqrt{2}-1)T^*$. For these small preview times, the cost reduces linearly in T. Only minor improvements in the cost are obtained for preview times $(\sqrt{2}-1)T^* < T \leq T^*$.

Preview Time	Optimal Cost, $p(T)$	Optimal Input, $u(t)$
$T \leq (\sqrt{2}-1)T^*$	$\frac{\bar{d}^2}{2rb} - \bar{d}T$	Equation 3
$(\sqrt{2}-1)T^* < T \leq T^*$	$\frac{br}{16}\frac{(-T^2+2TT^*+T^{*2})^2}{(T+T^*)^2}$	Equation 5
$T > T^*$	$\frac{\bar{d}^2}{16rb}$	Equation 6

TABLE I
SUMMARY OF RESULTS FOR $a = 0$

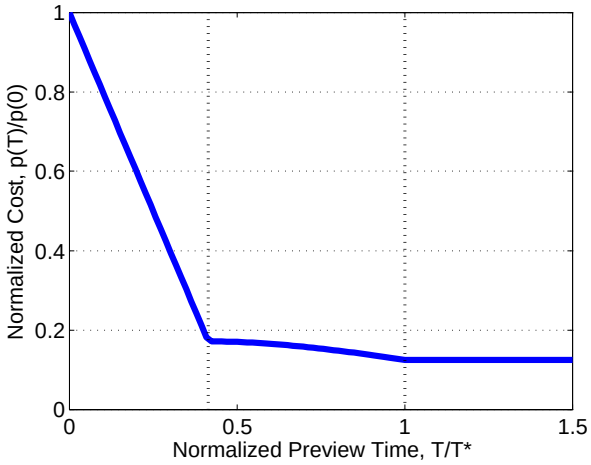

Fig. 3. Normalized performance versus normalized preview time

V. Optimal Response For $a > 0$

This section considers the case where the system is strictly stable ($a > 0$) and proves the following result: there exists $\bar{T}$ such that $p(T) = p(\bar{T})\ \forall T \geq \bar{T}$. In other words, the actuator rate constraint places a fundamental bound on tracking performance that cannot be overcome with preview.

A. Long Preview Response

The first step is to determine $\bar{T}$ and construct a candidate optimal input $\bar{u}$ and state response $\bar{x}$ for preview time $T = \bar{T}$. The response for $a = 0$ and $T = T^*$ (dash-dotted curve in Figure 2) displays the basic features of the expected solution. Based on these features, the optimal input for $a > 0$ and $T = \bar{T}$ is expected to have the form:

$$\bar{u}(t) = \begin{cases} +rt & \text{if } t < t_1 \\ -r(t-2t_1) & \text{if } t_1 \leq t < t_3 \\ \bar{u}(t_3) & \text{if } t \geq t_3 \end{cases} \tag{7}$$

for some t_1 and t_3. In addition, the optimal state response is expected to satisfy the following constraints:

- $\bar{x}(t_2) = +\bar{p}$ and $\dot{\bar{x}}(t_2) = 0$
- $\bar{x}(\bar{T}) = -\bar{p}$
- $\bar{x}(t_3) = +\bar{p}$ and $\dot{\bar{x}}(t_3) = 0$

where $t_2 < \bar{T} < t_3$ and $\bar{p}$ is the peak tracking error. This set of five constraints on $\bar{x}(t)$ and $\dot{\bar{x}}(t)$ can be solved for the five unknowns $(t_1, t_2, \bar{T}, t_3, \bar{p})$. Solving these equations requires explicitly integrating the state dynamics (Equation 1).

These constraint equations can be solved after lengthy but straightforward algebra. Recall $T^* := \frac{\bar{d}}{rb}$ and define the non-dimensional constants $\alpha := aT^*$ and $\beta := \frac{\alpha}{e^\alpha - 1}$. The five unknowns of the candidate optimal solution are given by:

$$t_1 := -\frac{T^*}{\alpha}\log\left(1 - \sqrt{1 - e^{-\frac{1}{2}(\beta - 1 - \log\beta)}}\right) \tag{8}$$

$$t_2 := 2t_1 - \frac{T^*}{2\alpha}(\beta - 1 - \log\beta) \tag{9}$$

$$\bar{T} := t_2 - \frac{T^*}{\alpha}\log\beta \tag{10}$$

$$t_3 := t_2 + T^* \tag{11}$$

$$\bar{p} = \frac{\bar{d}T^*}{2\alpha^2}(\beta - 1 - \log\beta) \tag{12}$$

For given $a, b, \bar{d} > 0$, the equations define a preview time $\bar{T}$ and a feasible input $\bar{u}$ that achieves the cost $\bar{p}$. The limits of these values as $a \to 0$ agree the results presented in the previous section for $a = 0$ and $T = T^*$. This feasible solution provides a bound on the optimal performance.

Lemma 1: $p(T) \leq \bar{p}\ \forall T \geq \bar{T}$.

Proof: Equations 8-12 define an input $\bar{u}$ and state $\bar{x}$ that achieve a cost $\|\bar{x}\|_\infty = \bar{p}$ for preview time $\bar{T}$. Therefore $p(\bar{T}) \leq \bar{p}$. Moreover, the performance $p(T)$ is a monotonic function of preview time: $p(T) \leq p(\bar{T})\ \forall T \geq \bar{T}$. ■

Figure 4 shows the state response and input for the data $a = 2$, $b = 1$, $r = 16$, and $\bar{d} = 16$. For this data, $t_1 \approx 0.308$sec, $t_2 \approx 0.497$sec, $\bar{T} \approx 1.078$sec, and $t_3 \approx 1.497$sec. The vertical lines in Figure 4 are drawn at these four times. In addition, $\bar{p} \approx 0.949$. The two horizontal lines in the top subplot of Figure 4 are drawn at $\pm\bar{p}$. For comparison, the optimal response for $a = 0$, $b = 1$, $r = 16$, and $\bar{d} = 16$ (shown in Figure 2) is given by: $t_1 = 0.25$sec, $t_2 = 0.50$sec, $T^* = 1.0$sec, $t_3 = 1.50$sec, and $\bar{p} = 1.0$.

B. Lagrange Duality

Lagrange duality theory is used to prove that the candidate solution constructed in the previous subsection is in fact optimal. The primal/dual theory presented here essentially

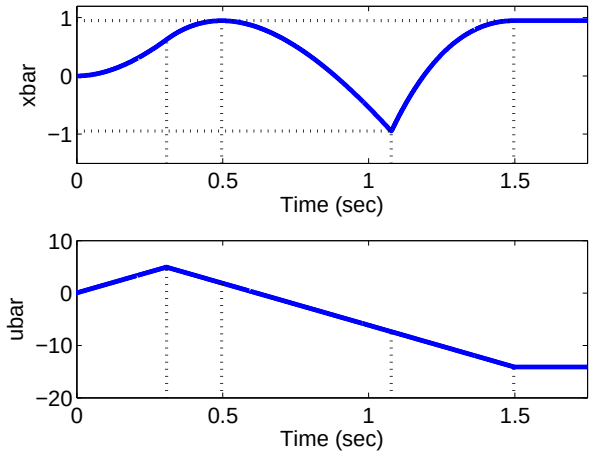

Fig. 4. Time responses of $\bar{x}(t)$ and $\bar{u}(t)$ for $a > 0$ and $T = \bar{T}$

relies on the results in [8]. Given $T_f < \infty$, define the vector spaces $Y := \mathbb{R} \times C[0, T_f]$ and $Z := C^4[0, T_f]$. Also define the functions $f : Y \to \mathbb{R}$ and $G : Y \to Z$ by:

$$f(\gamma, \dot{u}) = \gamma \tag{13}$$

$$G(\gamma, \dot{u}) = \begin{bmatrix} x - \gamma \\ -x - \gamma \\ \dot{u} - r \\ -\dot{u} - r \end{bmatrix} \tag{14}$$

where $x(t) = \int_0^t e^{-a(t-\tau)} \left(bu(\tau) + d_T(\tau) \right) d\tau$. f and G are both affine functions of $(\gamma, \dot{u})$ and hence they are convex. The optimal control problem in Equation 2 is formulated on an infinite horizon. A finite-horizon version of this problem expressed in terms of the vector space notation is:

$$\inf_{\substack{(\gamma, \dot{u}) \in Y \\ G(\gamma, \dot{u}) \leq 0}} f(\gamma, \dot{u}) \tag{15}$$

$G(\gamma, \dot{u}) \leq 0$ represents four infinite-dimensional linear constraints, e.g. the third constraint is $\dot{u}(t) \leq r \ \forall t \in [0, T_f]$. The optimization depends on the preview T through the state trajectory $x(t)$ that appears in the constraint function G.

The Lagrange duality result is based on a dual functional defined on the dual space of Z. By the Riesz representation theorem [8], $Z^* := NBV^4[0, T_f]$ is the dual space of $Z := C^4[0, T_f]$. Recall the positive cone $P^* \subset Z^*$ is defined as the set of functions $z^* \in NBV^4[0, T_f]$ such that each z_i^* is a nondecreasing function on $[0, T_f]$. The dual functional $\phi(z^*) : P^* \to \mathbb{R}$ for the vector space optimization (Equation 15) is defined by:

$$\phi(z^*) = \inf_{(\gamma, \dot{u}) \in Y} \left[f(\gamma, \dot{u}) + \sum_{i=1}^{4} \int_0^{T_f} g_i(t) dz_i^*(t) \right] \tag{16}$$

where g_i is the i^{th} entry of $G(\gamma, \dot{u})$.[2] The following Lagrange duality theorem [8] holds for the optimization in Equation 15.

[2]If $z_i^* \geq 0$ is everywhere differentiable with $\lambda_i(t) := \dot{z}_i^*(t)$ then $\lambda_i(t) \geq 0 \ \forall t$ and the Stieltjes integral $\int_0^{T_f} g_i(t) dz_i^*(t)$ is equivalent to $\int_0^{T_f} g_i(t) \lambda_i(t) dt$. This form is a natural extension of the Lagrange multiplier λ_i that appears in a finite-dimensional linear program. However, z_i^* is, in general, not differentiable.

Theorem 1: Suppose there exists $(\gamma_1, \dot{u}_1)$ such that $G(\gamma_1, \dot{u}_1) < 0$ and suppose the infimum in Equation 15 is finite. Then

$$\inf_{\substack{(\gamma, \dot{u}) \in Y \\ G(\gamma, \dot{u}) \leq 0}} f(\gamma, \dot{u}) = \max_{z^* \geq 0} \phi(z^*) \tag{17}$$

The maximum on the right is achieved by some $z_0^* \geq 0$.

If the infimum on the left is achieved by some $(\gamma_0, \dot{u}_0)$ then $\int_0^{T_f} g_{i,0}(t) dz_{i,0}^*(t) = 0$ for each i where $g_{i,0}$ is the i^{th} entry of $G(\gamma_0, \dot{u}_0)$.

The formulation of the optimization using the function space $C[0, T_f]$ ensures the existence of $(\gamma_1, \dot{u}_1)$ such that $G(\gamma_1, \dot{u}_1) < 0$. Specifically, the condition $G(\gamma_1, \dot{u}_1) < 0$ is satisfied by $\dot{u}_1(t) = 0 \ \forall t \in [0, T_f]$ and γ_1 sufficiently large. The finiteness of the infimum in Equation 15 follows from the existence of this feasible point and the fact that $\gamma \geq 0$ for any feasible point $(\gamma, \dot{u})$.

A simpler form of the dual optimization can be derived. Let $D \subset NBV^2[0, T_f]$ denote functions w^* that satisfy $TV(w_1^*) = 1$, w_2^* is everywhere differentiable, and

$$\frac{dw_2^*}{dt} = -\int_t^{T_f} h(\tau) d\tau \tag{18}$$

where $h(t) := \int_t^{T_f} be^{-a(\tau - t)} dw_1^*(\tau)$. Define the functional $\psi : D \to \mathbb{R}$ by:

$$\psi(w^*) = \int_T^{T_f} \frac{\bar{d}}{a} \left(1 - e^{-a(t-T)} \right) dw_1^*(t) - r \cdot TV(w_2^*) \tag{19}$$

ψ can be used to obtain a bound on the dual optimization.

Lemma 2: For any $w^* \in D$,

$$\psi(w^*) \leq \max_{z^* \geq 0} \phi(z^*) \tag{20}$$

Proof: Substituting for the g_i in the dual function (Equation 16) and re-arranging terms yields:

$$\begin{aligned} \phi(z^*) = \inf_{(\gamma, \dot{u}) \in Y} \gamma \left[1 - \int_0^{T_f} dz_1^*(t) - \int_0^{T_f} dz_2^*(t) \right] \\ -r \left[\int_0^{T_f} dz_3^*(t) + \int_0^{T_f} dz_4^*(t) \right] \\ + \int_0^{T_f} \dot{u}(t) dz_3^*(t) - \int_0^{T_f} \dot{u}(t) dz_4^*(t) \\ + \int_0^{T_f} x(t) dz_1^*(t) - \int_0^{T_f} x(t) dz_2^*(t) \end{aligned} \tag{21}$$

Define $\tilde{\psi} : NBV^2[0, T_f] \to \mathbb{R}$ by:

$$\begin{aligned} \tilde{\psi}(w^*) = \inf_{(\gamma, \dot{u}) \in Y} \gamma \left[1 - TV(w_1^*) \right] - r \cdot TV(w_2^*) \\ + \int_0^{T_f} \dot{u}(t) dw_2^*(t) + \int_0^{T_f} x(t) dw_1^*(t) \end{aligned} \tag{22}$$

Any $w_1^* \in NBV[0, T_f]$ can be decomposed as $w_1^* := z_1^* - z_2^*$ such that z_1^* and z_2^* are monotone non-decreasing functions with $TV(w_1^*) = TV(z_1^*) + TV(z_2^*)$ [11]. w_2^* can be similarly decomposed as $z_3^* - z_4^*$. For any $w^* \in NBV^2[0, T_f]$ this decomposition defines a $z^* \in P^*$ such that $\tilde{\psi}(w^*) = \phi(z^*)$. Thus it follows that:

$$\tilde{\psi}(w^*) \leq \max_{z^* \geq 0} \phi(z^*) \tag{23}$$

After substituting for $x(t)$ and re-arranging the integrals, $\tilde{\psi}$ can be written as:

$$\begin{aligned}\tilde{\psi}(w^*) = &\inf_{(\gamma,\dot{u})\in Y} \gamma\left[1 - TV(w_1^*)\right] - r \cdot TV(w_2^*) \\ &+ \int_T^{T_f} \tfrac{\bar{d}}{a}\left(1 - e^{-a(t-T)}\right) dw_1^*(t) \\ &+ \left[\int_0^{T_f} \dot{u}(t) dw_2^*(t) + \int_0^{T_f} u(t)h(t)dt\right]\end{aligned} \tag{24}$$

If $TV(w_1^*) = 1$ and $\frac{dw_2^*}{dt} = -\int_t^{T_f} h(\tau)d\tau$ then terms involving γ, u, and $\dot{u}$ are zero. Thus $\tilde{\psi}(w^*) = \psi(w^*)$ for all $w^* \in D$. ∎

This lemma can be strengthened. It can be shown that $\tilde{\psi}(w^*)$ is finite if and only if $w^* \in D$. In addition, the dual optimization can be equivalently reformulated in terms of ψ.

$$\max_{z^*\geq 0} \phi(z^*) \;=\; \max_{w^*\in D} \psi(w^*) \tag{25}$$

These stronger results require technical steps that are omitted since they are not required for the remainder of the paper.

C. Main Result

Theorem 2: Let $a, b, \bar{d}, r > 0$ be given and consider the optimal disturbance rejection problem in Equation 2. There exists $\bar{T}$ such that $p(\bar{T}) > 0$ and $p(T) = p(\bar{T})\ \forall T \geq \bar{T}$.

Proof: Equations 8-12 define a feasible input achieving a cost $\bar{p} > 0$. By Lemma 1, $p(T) \leq \bar{p}\ \forall T \geq \bar{T}$. The proof is completed by showing that $p(T) \geq \bar{p}\ \forall T \geq \bar{T}$.

By Theorem 1 and Lemma 2, if $w^* \in D$ then $\psi(w^*)$ provides a lower bound on the the finite horizon optimization (Equation 15). For any preview time T and horizon time $T_f < \infty$, the finite-horizon problem (Equation 15) provides a lower bound on the infinite-horizon cost $p(T)$. This follows because infinite-horizon solutions can be truncated to give feasible solutions on $[0, T_f]$ without increasing the cost. Thus $\psi(w^*) \leq p(T)$ for any $T_f < \infty$ and any $w^* \in D$.

First consider $T = \bar{T}$ and choose any $T_f \geq t_3$. Define w_1^* and $\dot{w}_2^*$ by:

$$w_1^*(t) = \begin{cases} 0 & \text{if } t < t_2 \\ \frac{1}{2} - c & \text{if } t_2 \leq t < T \\ -c & \text{if } T \leq t < t_3 \\ 0 & \text{if } t_3 \leq t \end{cases} \tag{26}$$

$$\dot{w}_2^*(t) = \begin{cases} 0 & \text{if } t < t_2 \\ \frac{-b(1-2c)}{2a}\left[e^{a(t-t_2)} - 1\right] & \text{if } t_2 \leq t < T \\ \frac{-bc}{a}\left[1 - e^{a(t-t_3)}\right] & \text{if } T \leq t < t_3 \\ 0 & \text{if } t_3 \leq t \end{cases} \tag{27}$$

where $c := \frac{1-\beta}{2(1-e^{-\alpha})}$. w_2^* is obtained by integrating Equation 27 with initial condition $w_2^*(0) = 0$. This yields a $w^* \in NBV^2[0, T_f]$. It can be verified that $w^* \in D$ and $\psi(w^*) = \bar{p}$. Thus $p(\bar{T}) \geq \psi(w^*) = \bar{p}$.

This w^* can be time-shifted for the case $T \geq \bar{T}$. Specifically, for any $T \geq \bar{T}$ choose $T_f \geq t_3 + (T - \bar{T})$. Define the dual variable $\tilde{w}^*(t) = 0$ for $t \leq (T - \bar{T})$ and $\tilde{w}^*(t) = w^*(t - (T - \bar{T}))$ otherwise. This gives $\psi(\tilde{w}^*) = \bar{p}$ for any $T \geq \bar{T}$. Hence $p(T) \geq \bar{p}\ \forall T \geq \bar{T}$. ∎

The construction of the dual variable w^* is based on the alignment condition $\int_0^{T_f} g_{i,0}(t)dz_{i,0}^*(t) = 0$ in Theorem 1. If this condition holds then $z_{i,0}$ can only vary, at most, on the set of times where $g_{i,0}(t) = 0$. The candidate solution $\bar{x}$ only achieves its peak magnitude at times t_2, T, and t_3. For this solution, $g_{1,0}(t) = 0$ only at $t = t_2$ and t_3 and $g_{2,0}(t) = 0$ only at $t = T$. Since $w_1^* = z_1^* - z_2^*$, w_1^* is constructed to be a step function with increasing jumps at $t = t_2$ and t_3 and a decreasing jump at $t = T$. w_2^* can be computed from w_1^* using Equation 18. Thus the construction of w^* reduces to determining the values of the three discontinuous jumps in w_1^*. The jump magnitudes can be determined from the constraint $TV(w_1^*) = 1$ and by imposing $\dot{w}_2^*(t) = 0$ for $t \leq t_2$. The condition on $\dot{w}_2^*$ can be inferred from the structure of the optimal input for $T > T^*$.

VI. Conclusions

This paper considered a regulation problem with disturbance preview information and actuator rate constraints. Lagrange duality theory was used to derive explicit formulas for the optimal control action. The optimal performance as a function of preview time was also provided. There is a fundamental preview time beyond which no performance improvements are obtained. It would be interesting to compare model predictive control with this explicit optimal control.

VII. Acknowledgments

This work was supported by the Institute for Renewable Energy and the Environment under Project No. RL-0010-12 entitled "Design Tools for Multivariable Control of Large Wind Turbines."

References

[1] M. Donahue. Implementation of an active suspension, preview controller for improved ride comfort. Master's thesis, University of California, Berkeley, 2001.

[2] F. Dunne, L. Pao, A. Wright, B. Jonkman, N. Kelley, and E. Simley. Adding feedforward blade pitch control for load mitigation in wind turbines: Non-causal series expansion, preview control, and optimized FIR filter methods. In *49th AIAA Aerospace Sciences Meeting*, number AIAA-2011-819, 2011.

[3] A. Koerber and R. King. Nonlinear model predictive control for wind turbines. In *Proceedings of the 2011 EWEA Annual Event*, 2011.

[4] A. Kojima and S. Ishijima. H_∞ performance of preview control systems. *Automatica*, 39:693–701, 2003.

[5] J. Laks, L. Pao, E. Simley, A. Wright, and N. Kelley. Model predictive control using preview measurements from LIDAR. In *49th AIAA Aerospace Sciences Meeting*, number AIAA-2011-813, 2011.

[6] J. Laks, L. Pao, and A. Wright. Combined feed-forward/feedback control of wind turbines to reduce blade flap bending moments. In *47th AIAA Aerospace Sciences Meeting*, number AIAA-2009-687, 2009.

[7] J. Laks, L. Pao, A. Wright, N. Kelley, and B. Jonkman. Blade pitch control with preview wind measurements. In *48th AIAA Aerospace Sciences Meeting*, number AIAA-2010-251, 2010.

[8] D. Luenberger. *Optimization by Vector Space Methods*. John Wiley & Sons, 1969.

[9] A.A. Moelja and G. Meinsma. H_2 control of preview systems. *Automatica*, 42:945–952, 2006.

[10] A. Ozdemir, P. Seiler, and G. Balas. Fundamental limitations of preview for wind turbine control. In *Submitted to the 50th AIAA Aerospace Sciences Meeting*, 2012.

[11] H. L. Royden. *Real Analysis*. Macmillan Publishing, 1988.

[12] M. Tomizuka and D.E. Rosenthal. On the optimal digital state vector feedback with integral and preview actions. *ASME J. of Dyn. Systems, Meas., and Control*, 101:172–178, 1979.